IEEE Access
Multidisciplinary | Rapid Review | Open Access Journal

Received August 13, 2019, accepted August 31, 2019, date of publication September 16, 2019,
date of current version September 30, 2019.

Digital Object Identifier 10.1109/ACCESS.2019.2941539

Mesh Adaptation Method for Optimal Control With Non-Smooth Control Using Second-Generation Wavelet

ZHIWEI FENG, QINGBIN ZHANG, JIANQUAN GE, WUYU PENG, TAO YANG, AND JINLIANG JIE

College of Aerospace Science and Engineering, National University of Defense Technology, Changsha 410073, China

Corresponding author: Qingbin Zhang (qingbinzhang@sina.com)

This work was supported by the National Natural Science Foundation of China under Grant 11772353.

ABSTRACT A mesh adaptation method is proposed for solving optimal control problems with non-smooth control. The original optimal control problem (OCP) is transcribed into a nonlinear programming (NLP) problem by using the Runge-Kutta discretization method, in which the NLP can be solved by using standard nonlinear programming codes. The method employs collocations from the dyadic background points, which used for the second-generation wavelet (SGW) translation simultaneously. The SGW is used to approximate the control variables and get the wavelet coefficients once they are obtained. In regions contain discontinuities, the magnitude of the relevant wavelet coefficients is large than other regions. The corresponding dyadic background points are reserved as the collocation points. Furthermore, the approximation error of the control and/or state variables can be predicted by a given threshold. Thus, the accuracy and efficiency can be balanced in a simple way. Finally, the method is demonstrated by three numerical examples from the open literature.

INDEX TERMS Optimal control, mesh adaptation, adaptive collocation method, second generation wavelets.

I. INTRODUCTION

Numerical method of optimal control has wide spread application in aerospace field, such as flight trajectory optimization, missile guidance, orbit transfer, et al. For these nonlinear optimal control problems, although various control methods have been developed [1], [2], the direct transcription method is a general method. For the direct transcription method, the original optimal control problems are translated into nonlinear programming (NLP) problem, and solved using the well-known NLP algorithm [3]. There has been developed various method to solve optimal control problems numerically, i.e. multi-shooting method [4], direct collocation method [5], pseudospectral method [6] and others. To achieve the desired accuracy, the computational mesh is often adjusted according to the estimated control or state variables, and multiple iterations are required. Therefore, mesh adaptation method is important for high precision solution of the optimal control problems.

The associate editor coordinating the review of this manuscript and approving it for publication was Jianxiang Xi.

Various mesh adaptation method has been proposed to deal with the contradiction between the accuracy and efficiency for numerically solving optimal control problems. The mesh adaptation method used in SOCS is based on integer programming, and the goal is to minimize the maximum integration error in the mesh adaptation process [7]. Ross and Fahroo proposed the pseudospectral knotting method, in which the original optimal control problem is divided into multiple phases by discontinuity point of control, and add linkage constraints [8]. In each phase, the pseudospectral (PS) method is employed to obtain the discretization nonlinear programming problem. Darby, Hagar et al proposed the hp-adaptive method, in which the method starts with a global pseudospectral approximation, and then iteratively determines the number of segments, the width of each segment, and the degree of the polynomial in each segment until a specified error tolerance is satisfied [9]. In another literature, they proposed an adaptive mesh adaptation method using the idea of non-smoothness detection and mesh size reduction [10]. The fundamental idea in above method is to redistribute the mesh points according to the local integration

or interpolation error. In addition, an intuitional strategy is to use locally dense mesh in the region of discontinuities for the control function or its higher order derivatives. A mesh adaptation method using multi-resolution analysis is proposed in literature [11]. The method is based on the interpolating wavelets. The error can be estimated about the local smoothness of the solution in this method. The density function method employs this strategy [12], and the redistribution of mesh points is achieved by using the density function which reflect the non-smoothness in the control function and its higher order derivatives. For specific problems, some mesh adaptive methods are also proposed, such as the adaptive Gauss pseudospectral method for hypersonic re-entry vehicle problem [13], mesh adaption for nonlinear model predictive control [14], and the sensitivity-based adaptative mesh adaptation for chemical and biochemical process [15].

Mesh adaptation is a common topic in other areas. The wavelet adaptive method for mesh adaptation has been used in the computation fluid dynamics where capturing the fine structure of the fluid field is required. Despite their popularity in other fields, the wavelet adaptive method has rarely been used for optimal control problems. Second generation wavelet functions have well time/frequency local property, which are suitable for fitting the function with localized structures or sharp transitions. The second-generation wavelet collocation method has been proposed to construct non-uniform space grids in time iteration step [16] for solving partial differential equations with sharp transitions. In numerical optimal control, there are a lot of problems whose control functions are discontinuous. The second-generation wavelet collocation method can also be applied to the optimal control problem with discontinuous control.

Based on the above idea, we propose a novel mesh adaptation method for numerically solving optimal control problems. The optimal control problem is transcribed into a nonlinear programming (NLP) problem by using the Runge-Kutta discretization method. The mesh adaptation algorithm iteratively determines the suitable non-uniform grid, over which the optimal control problem is discretized and solved iteratively. Based on the magnitude of the wavelet coefficients, more grid points around the discontinuity of the control variables or the non-smoothness of the state variables would be placed. The method uses a sequential optimization technology, the process will end until the desired accuracy is satisfied.

Compared to the multi-resolution analysis-based mesh adaptation method, the second-generation wavelet has well global characteristic than interpolating wavelets. Therefore, the distribution of adaptive grid would be more reasonable, and can balance both the global of local feature of control variables. Compared to the integration error based method, the proposed method can not only increase the points, but also remove points around the region the control variables are gently changed. It would be more effective potentially.

The paper is organized as follows. In Section II, the optimal control problem is formulated, and the continuous optimal control problem is transcribed into an NLP problem. In Section III, second generation wavelets are described, and the mesh adaptation algorithm for solving optimal control problems is proposed. In Section IV, several applications of the proposed method are provided. Finally, in Section V, the concluding remark is provided.

II. PROBLEM FORMULATION

A. OPTIMAL CONTROL PROBLEM

In order to give a basic description, consider the following optimal control problem. Determine the control function $u(\cdot)$ and corresponding state function $x(\cdot)$ that minimize the Mayer cost function:

$$J\left[x(\cdot), u(\cdot), t_f\right] = M\left[x\left(t_f\right), t_f\right] \tag{1}$$

where $t \in \left[t_0, t_f\right]$, $x \in \mathrm{R}^n$, $u \in \mathrm{R}^m$, $M : \mathrm{R}^n \times \mathrm{R} \to \mathrm{R}$, and $L : \mathrm{R}^n \times \mathrm{R}^m \times \mathrm{R} \to \mathrm{R}$. Subject to the state dynamics

$$\dot{x}(t) = f(x(t), \quad u(t), t) \tag{2}$$

the boundary conditions

$$\dot{x}(t_0) = x_0, \quad e_f\left(x\left(t_f\right), t_f\right) = 0 \tag{3}$$

where $e : \mathrm{R}^n \times \mathrm{R} \to \mathrm{R}^n$, and the constraints

$$\begin{cases} C_u(u(t)) \le 0 \\ C_x(x(t)) \le 0 \\ C_{xu}(x(t), u(t)) \le 0 \end{cases} \tag{4}$$

In most cases, the initial time t_0 is assumed to be given and the final time t_f can be fixed or free. The Bolza cost function can be converted into a Mayer cost function by adding a state and a differential equation [17].

Without loss of generality, we assume that the time interval is the unit interval, in other words, $t \in \left[t_0, t_f\right] = [0, 1]$. The transformation from $\left[t_0, t_f\right]$ to [0, 1] is well-known, thus the details are omitted.

Next, the transcription from the continuous optimal control problem over the interval [0, 1] to an NLP problem over grid points is described.

B. TRANSCRIPTION USING RUNGE-KUTTA METHOD

The optimal control problem can be converted into an NLP problem by using Runge-Kutta (RK) discretization. A K-stage Runge-Kutta scheme is given by [7].

$$x_{i+1} = x_i + h_i \sum_{j=1}^{K} \beta_j f_{ij} \tag{5}$$

where

$$f_{ij} = f\left[\left(x_i + h_i \sum_{l=1}^{K} \alpha_{jl} f_{jl}\right), \left(t_i + h_i \rho_j\right)\right] \tag{6}$$

for $1 \le j \le K$. K is the stage of RK method, and i is the time step. In above expressions, $\left\{\rho_j, \beta_j, \alpha_{jl}\right\}$ are known constants with $0 \le \rho_1 \le \rho_2 \ldots \le \rho_K \le 1$. A simple way to define the coefficients is to use the so-called Butcher

array [18]. The scheme is explicit if $\alpha_{jl} = 0$ for $l \geq j$ and implicit otherwise. The well-known examples of K-stage Runge-Kutta schemes are the trapezoidal method ($q = 2$), the Hermite-Simpson method ($q = 3$), and the classical fourth-order RK method ($q = 4$) [7].

Using Equation (5), the defects of the discretization are given by

$$\zeta_i = x_{i+1} - x_i - h_i \sum_{j=1}^{K} \beta_j f_{ij} \tag{7}$$

for $i = 0, ..., N-1$.

Let us now define the following sets: $X = \{x_0, ..., x_N\}$, $U = \{u_0, ..., u_N\}$, $\tilde{U} = \{\tilde{u}_0, ..., \tilde{u}_{N-1}\}$. Finally, the optimal control problem reduces to the following NLP problem in terms of the variables X, U, and $\tilde{U}$. Minimize

$$J = M(x(1)) \tag{8}$$

subject to the constraints

$$\zeta_i = 0, i = 0, ..., N-1 \tag{9}$$
$$x(0) = x_0 \tag{10}$$
$$e(x(1)) = 0 \tag{11}$$
$$C_u\left(U, \tilde{U}\right) \leq 0 \tag{12}$$
$$C_x(X) \leq 0 \tag{13}$$

Note that the convergence of the Runge-Kutta schemes for optimal control problems has been demonstrated by [19], [21]. In order to obtain consistent approximations and higher order accuracy of solution, the classical 4-stage explicit fourth-order Runge-Kutta schemes is used in this paper. This scheme satisfies all the conditions needed for fourth-order accuracy in optimal control given by [21].

The proposed mesh adaptation method for optimal control is based on the second-generation wavelet, which is mostly constructed on a set of uniform dyadic grids on the real line or interval. For consisted with the transcription method, an interval of [0, 1] is used in this paper. The adaptive grids are part of dyadic grids. The grid points of adaptive grids are determined according to the control or state variables, and desired approximation accuracy.

III. SECOND-GENERATION WAVELET BASED MESH ADAPTATION ALGORITHM

The mesh adaptation method is usually used to increase the accuracy of the solution for the optimal control problems. The adaptive wavelet collocation (AWC) method [16] based on second-generation wavelet is firstly introduced in this section. AWC is a common framework for constructing adaptive numerical methods for solving partial differential equation. This method is using the second-generation wavelet decomposition for mesh adaptation and finite difference. For numerical method of optimal control using the RK scheme, the mesh adaptation method based on AWC is proposed. The AWC is modified to reduce the mesh points.

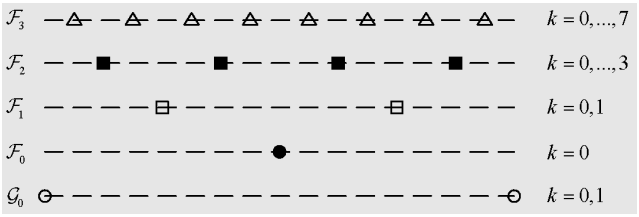

FIGURE 1. Example of dyadic grid.

A. DYADIC GRIDS AND MULTI-RESOLUTION ANALYSIS

The second-generation wavelets (SGW) are constructed on a set of dyadic grids. Because the mesh refine process is based on SGW, the discretization of the optimal control problem will be performed on a set of (non-uniform) grids taken from the dyadic grids. A uniform dyadic grid over the interval $I = [0, 1]$ is a collection of points of the form [22].

$$G_j = \left\{ t_k^j \in [0, 1] : t_k^j = k/2^j, 0 \leq k \leq 2^j \right\}, \quad J_0 \leq j \leq J \tag{14}$$

where j is the resolution level, k is the spatial location, J and J_0 are positive integers. Let $\mathcal{F}_j$ denote the set of grid points belonging to $\mathcal{G}_{j+1} \backslash \mathcal{G}_j$; that is

$$\mathcal{F}_j = \left\{ \tilde{t}_k^j \in [0, 1]; \tilde{t}_k^j = (2k+1)/2^{j+1}, 0 \leq k \leq 2^j - 1 \right\}, \quad J_{\min} \leq j \leq J_{\max} - 1 \tag{15}$$

It is obvious that

$$t_k^j = x_{2k}^{j+1} \in \mathcal{G}^j, \quad \tilde{t}_k^j = t_{2k+1}^{j+1} \in \mathcal{F}^j, \quad 0 \leq k \leq 2^j \tag{16}$$

and $\{\mathcal{G}_j\}$, $J_{\min} \leq j \leq J_{\max}$ forms a sequence of nested grid set, exactly $\mathcal{G}_{J_{\min}} \subset \mathcal{G}_{J_{\min}+1} \subset \cdots \subset \mathcal{G}_{J_{\max}}$. An illustration of one dimensional case is given in Figure 1.

Next, the definition of multi-resolution analysis is given briefly [22]. Definition: A second-generation multi-resolution analysis M of a function space L consists of a sequence of closed subspaces $M = \{\mathcal{V}_j \subset L | j \in \mathcal{J}\}$ so that

(1) $\mathcal{V}_j \subset \mathcal{V}_{j+1}$;

(2) $\cup_{j \in \mathcal{J}} \mathcal{V}_j$ is dense in L;

(3) for each $j \in \mathcal{J}$, $\mathcal{V}_j$ has a Riesz basis given by scaling functions $\left\{ \phi_k^j \,|k \in \mathcal{K}^j \right\}$. in which, $\mathcal{K}^j$ is some index set. Let the superscript j to denote the level of resolution and the subscript k to denote the location at that level of resolution for notational convenience. It is worth emphasizing that there is no limitation on ϕ_k^j to be dilated or translated from some fixed mother function. $\mathcal{W}^j$ is named as the complement of $\mathcal{V}^j$ in $\mathcal{V}^{j+1}$, i.e. $\mathcal{V}^{j+1} = \mathcal{V}^j \oplus \mathcal{W}^j$, and wavelet $\psi_k^j (l \in L^j)$ is the basis function for $\mathcal{W}^j$.

The multi-resolution decomposition from level J down to a coarser level J_0 is performed as

$$\mathcal{V}^J = \mathcal{V}^{J_0} + \mathcal{W}^{J_0} + \mathcal{W}^{J_0+1} + ... + \mathcal{W}^{J-1}, \quad J_0 \geq 0, J \geq 1 \tag{17}$$

So, we have the wavelet representation of a function as follows

$$f(x) \approx \sum_{k \in G^{J_0}} c_k^{J_0} \phi_k^{J_0}(t) + \sum_{J_0 \le j \le J-1} \sum_{k \in F^j} d_k^j \psi_k^j(t), \quad \forall t \in I \tag{18}$$

For the functions with isolated small scales on a large-scale background, the most coefficients are very small. For the second-generation wavelet, every wavelet is uniquely associated with a grid point, and thus grid adaption is simply based on the analysis of wavelet coefficients; i.e., at any given iteration step of solving for optimal control problem, the used grid points consist of points corresponding to wavelets whose coefficients are greater than a given threshold ε, which is the parameter controls the accuracy of the solution.

B. SECOND-GENERATION WAVELETS AND TRANSFORM

Second-generation wavelets are a generalization of bi-orthogonal wavelet, but not have the translation and dilation invariance of their bi-orthogonal companion. For completeness of presenting the mesh adaptation method for solving optimal control problem, second-generation wavelets are shortly introduced in this section. The completely and strictly discussion of second-generation wavelets can be found in [22] and [16].

In the multi-resolution analysis of second-generation wavelets, a function $f(t) \in L^2$ can be approximated on some certain level of J as follows

$$f^J(t) = \sum_{k \in G^{J_0}} c_k^{J_0} \phi_k^{J_0}(t) + \sum_{J_0 \le j \le J-1} \sum_{k \in F^j} d_k^j \psi_k^j(t), \quad \forall t \in I \tag{19}$$

where ϕ is the scaling function and ψ is wavelet function; c and d are scaling coefficient and wavelet coefficient. If the level of resolution J is high sufficiently such that all scales are adequately resolved, then the error $\|f(t) - f^J(t)\|_\infty$ can be negligible in the sense that it is of the same order truncation of the machine. Then $f^J(t)$ is given a good approximation of original function $f(t)$. For the mesh adaptation of optimal control problem, the function $f(t)$ can be state function or control function.

The tool for constructing second-generation is the lifting scheme. In contrast to classical wavelets, the advantage of lifting scheme is that the wavelets can be designed for interval and irregular sampling. The construction of second-generation wavelet involves two building blocks, interpolating and lifting. They are all based on local polynomial interpolation on dyadic grids $\{\mathcal{G}_j\}$. Given a sampling $\left\{f_k^j = f\left(t_k^j\right), \forall t_k^j \in \{\mathcal{G}_j\}\right\}$ of x, the basic procedure of constructing second-generation wavelet is predicting the function value of f on $\mathcal{F}_j$ by polynomial interpolation of degree $2N-1$ and then update the function value on $\mathcal{G}_j$ by polynomial interpolation of degree $2\tilde{N}-1$.

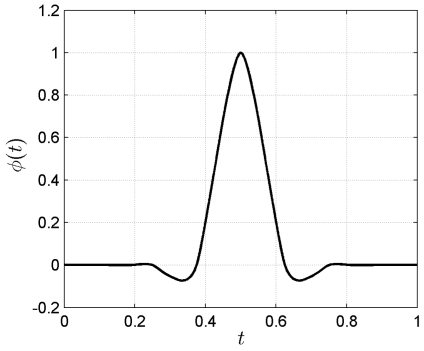

FIGURE 2. Scale function of lifted interpolating wavelet.

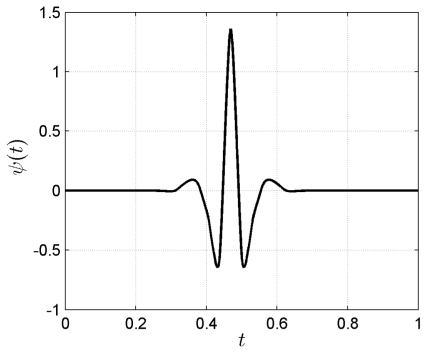

FIGURE 3. Wavelet function of lifted interpolating wavelet.

For the lifted interpolating wavelet, the forward wavelet transform can be depicted by [16], [22].

$$d_k^j = \frac{1}{2}\left(c_{j+1}^{2k+1} - \sum_l w_j^{k,l} c_{j+1}^{2k+2l}\right) \tag{20}$$

$$c_k^j = c_{2k+1}^{j+1} + \sum_l \tilde{w}_{k,l}^j d_{k+l}^j \tag{21}$$

while the inverse wavelet interpolating transform can be given by

$$c_{2k}^{j+1} = c_k^j - \sum_l \tilde{w}_{k,l}^j d_{k+l}^j \tag{22}$$

$$c_{2k+1}^{j+1} = 2d_k^j + \sum_l \tilde{w}_{k,l}^j c_{k+l}^j \tag{23}$$

where $w_{k,l}^j$ and $\tilde{w}_{k,l}^j$ are the interpolating coefficients from even points $t_{2(k+l)}^{j+1}$ to odd points t_{2k+1}^{j+1} and from odd points $t_{2k+2l+1}^{j+1}$ to even points t_{2k}^{j+1} respectively. The above coefficients can be determined by the lifting interpolating scheme. In the numerical implementation, there are three steps for forward wavelet transform, i.e. splitting, interpolating (or prediction), and lifting (or update) [22].

The order of interpolating polynomial used in this paper is $N = \tilde{N} = 2$, the corresponding interpolating weights and update weights are illustrated in Table 1 and Table 2. An example of scale function and wavelet function of the lifted interpolating wavelet is shown in Figure 2 and Figure 3.

TABLE 1. Interpolating weights for $N = 2$.

	1	2	3	4
Left boundary point	5/16	15/16	-5/16	1/16
Inner point	-1/16	9/16	9/16	-1/16
Right boundary point	1/16	-5/16	15/16	5/16

TABLE 2. Lifting weights for $\tilde{N} = 2$.

	1	2	3	4
Left boundary point1	35/16	-35/16	21/16	-5/16
Left boundary point2	5/16	15/16	-5/16	1/16
Inner point	-1/16	9/16	9/16	-1/16
Right boundary point2	1/16	-5/16	15/16	5/16
Right boundary point1	-5/16	21/16	-35/16	35/16

C. MESH ADAPTATIVE METHOD

For the optimal control problem with irregularities or discontinuities in the control function, it is desired to get an accurate solution with fewer collocation points. The basic idea is to use denser collocation around the discontinuities, and use sparse in other area. In this research, the second-generation wavelets and the mesh adaptative method based on it are employed to achieve this purpose.

Consider the control function $u(t)$ defined on a closed interval $[0, 1]$. The second-generation wavelets are constructed on a set of grids,

$$\mathcal{G}^j = \left\{ t_k^j \in \Omega : k \in \mathcal{K}^j \right\}, \quad j \in \mathcal{Z} \tag{24}$$

where grid points t_k^j can be uniformly or non-uniformly spaced, satisfying $t_k^j = t_{2k}^{j+1}$. The grid guarantees the nestingness, i.e., $G^{j-1} \subset G^j$. According to the construction method of the second-generation wavelets, $u(t)$ can be represented approximately by scale function $\phi_k^j(t)$ $\left(k \in \mathcal{K}^j\right)$ and wavelet $\psi_l^j(t)$ $\left(l \in \mathcal{L}^j\right)$ such that on each level of resolution [21],

$$u^J(\tau) = \sum_{k \in \mathcal{K}^0} c_k^0 \phi_k^0(\tau) + \sum_{j=0}^{J-1} \sum_{l \in \mathcal{L}^j} d_l^j \psi_l^j(\tau) \tag{25}$$

The absolute of the wavelet coefficients represent the local smooth property of a function. If the function is smooth in local, then the corresponding wavelets coefficient will small. For the function with local irregularities or discontinuities, most of the coefficients will be small excepting that around the irregularities. Therefore, well approximation can be achieved even though discarding wavelets with small coefficient.

The approximation based on the second-generation wavelets can be denoted as a sum of two terms contains wavelets whose coefficients are above and below the given threshold ε [21].

$$u^J(t) = u_{\geq}^J(t) + u_{<}^J(t) \tag{26}$$

in which

$$u_{\geq}^J(\tau) = \sum_{k \in \mathcal{K}^0} c_k^0 \phi_k^0(\tau) + \sum_{j=0}^{J-1} \sum_{l \in \mathcal{L}^j, \left|d_l^j\right| \geq \varepsilon} d_l^j \psi_l^j(\tau) \tag{27}$$

$$u_{<}^J(\tau) = \sum_{j=0}^{J-1} \sum_{l \in \mathcal{L}^j, \left|d_l^j\right| < \varepsilon} d_l^j \psi_l^j(\tau) \tag{28}$$

According to the above approximation, all grid points t_k^j associated with wavelets $\left|d_i^j\right| > \varepsilon$ are collected, i.e.

$$\mathcal{G}_\varepsilon^j = \left\{ t_k^j \in \Omega \,\middle|\, k \in \mathcal{K}^j, \left|d_i^j\right| > \varepsilon \right\} \tag{29}$$

It is noted that for a function with localized structures or non-smoothness, the number of $\mathcal{G}_\varepsilon^j$ would be much small than that of $\mathcal{G}^j$. Each scaling function $\phi_k^j(t)$ is uniquely associated with t_k^j, while each wavelet $\psi_k^j(t)$ is uniquely associated with t_{2l+1}^j. Therefore, after the wavelet decomposition, each grid point on $\mathcal{G}^J$ is associated with either the wavelet or the scaling function at the coarsest level of resolution. According these relations, the fewest grid points can be determined. Besides, the points associated with wavelets belonging to an adjacent zone should be included in the computational grid in order to improve the accuracy of the solution [16]. It is said that the wavelet $\psi_l^{j'}(t)$ belongs to the adjacent zone of wavelet $\psi_l^j(t)$, if they satisfy the following relations,

$$\left|j - j'\right| < L, \qquad \left|2^{j-j'} - k\right| < M \tag{30}$$

where L determines the level of resolution extent to, and M defines the width of the adjacent zone in the same level of resolution.

Given the value on finest grid $\mathcal{G}^J$ of control function u_k^J, the procedure for obtaining the new grid points based on adaptive method is as follows.

(1) Perform the forward wavelet transform on u_k^J, obtain the scaling coefficients c_k^0 $(k \in K)$ and the wavelet coefficients d_l^j $(l \in L, 0 \leq j \leq J-1)$ on each resolution level.

(2) Analyses wavelet coefficients for control function, and create a mask $\mathcal{M}$ for the grid points t_k^j associated with wavelets which have magnitude $\left|d_l^j\right|$ larger than ε.

(3) Extend the mask $\mathcal{M}$ to the grid points in the adjacent zone.

(4) Increment j by 1, then according to the above the mask $\mathcal{M}$ construct the computational grid points G_ε^j which will be used for the next step of optimization.

In the above step, the method adaptively removes the grid points from the region where the solution is smooth at the coarser level, and adds new grid points for the region where the previous control function has non-smoothness.

The compression and reconstruction of the smooth function with sharp transitions are tested with the following two functions.

TABLE 3. Approximation error for test function 1.

ε	$\left\|f(t)-f^J(t)\right\|_\infty$	N	$J_{\max}$
10-1	2.07 × 10-2	29	7
10-2	5.15 × 10-4	53	9
10-3	1.32 × 10-4	65	9
10-4	1.37 × 10-5	109	10
10-5	1.28 × 10-6	157	11
10-6	1.53 × 10-7	265	12

TABLE 4. Approximation error for test function 2.

ε	$\left\|f(t)-f^J(t)\right\|_\infty$	N	$J_{\max}$
10-1	6.25 × 10-2	46	12
10-2	2.47 × 10-4	75	12
10-3	2.22 × 10-6	83	12

(1) smooth function with local structure

$$f(x) = -\tanh\left((x - x_0)/\mu\right) \tag{31}$$

(2) discontinuities function common in bang-bang control

$$f(x) = \begin{cases} 0 & 0 \le x \le 0.5 \\ 1 & 0.5 < x \le 1 \end{cases} \tag{32}$$

The distribution of the significant wavelet coefficients $\left|d_k^j\right| \ge \varepsilon$ with $J_0 = 3, J = 12, N = \tilde{N} = 2, L = M = 1$ and $\varepsilon = 10^{-3}$ is plotted in Figure 4. For the first test, the max level of resolution is 9, the number of significant wavelet coefficients is 65; for the second test, the max level of resolution is 12, the number of significant wavelet coefficients is 83. Table 3 and Table 4 gives the approximation error (maximum norm of error function), retained number of wavelet coefficients and max level of resolution for the two test functions.

D. ITERATIVE PROCEDURE

Using the mesh adaptation method described above, the grid points automatically adapt to any non-smoothness in the control function. The procedure for solving optimal control problem is as follows:

Step1: Initialization

Set the coarsest and finest level of resolution J_0, and $J_{\max}$, the threshold ε, and wavelet adjacent parameter L and M.

Give an initial guess for state x and control u associated with collocation points on $\mathcal{G}^{J_0}$.

Set the stop condition, $j > J_{\max}$ or the grid points are the same for two close iterations.

Step2: Solve the NLP problem given by Runge-Kutta transcription method with the initial guess using some well-known methods, i.e. SNOPT [23], obtain the solution (state and control function).

Step3: Using the mesh adaptative method described in Section 3.3, obtain the new computational grid points G_ε^j. If the optimal control problem has multiple control variables, the grid points G_ε^j for each control variable are combined to a set of grid points.

Step4: Construct the new initial guess solution for G_ε^j.

Step5: If the stop condition is satisfied, output the state and control; otherwise go to **Step2**.

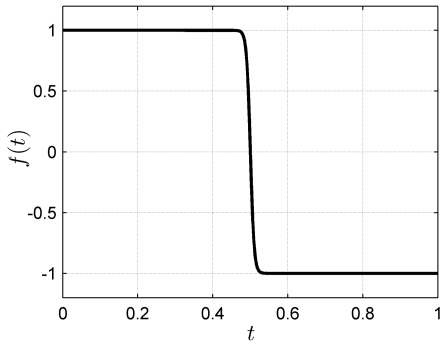

(a) Test function 1

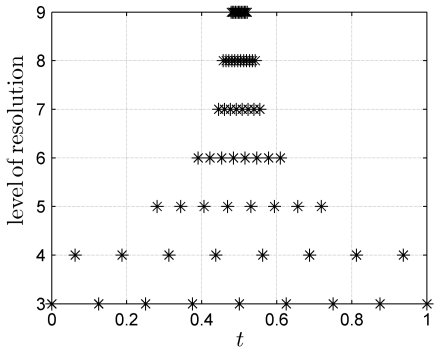

(b) Distribution of retained collocation points

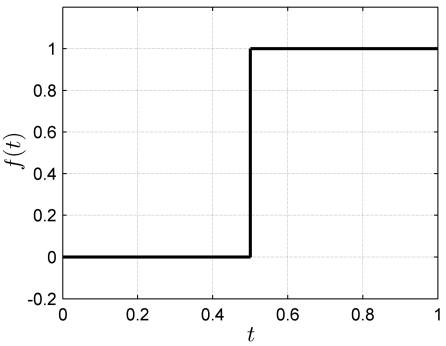

(c) Test function 2

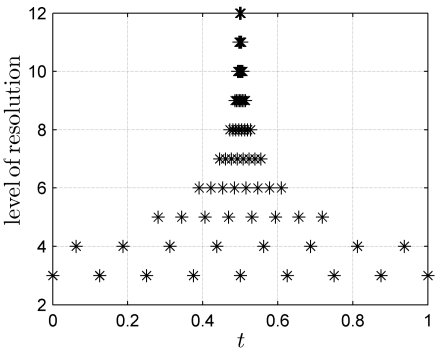

(d) Distribution of retained collocation points

FIGURE 4. Test function and grid points distribution.

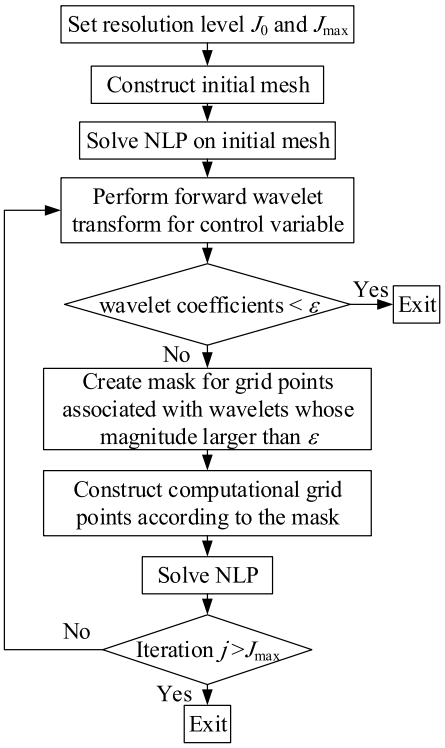

FIGURE 5. Schematic of mesh adaptation method using second generation wavelet (AWC-OC).

In Step1, the solution should converge fast, because the NLP problem was solved on the coarsest grid with fewest grid points. However, this rough solution on the coarsest grid may not be accurate enough. In order to improve the accuracy close to the control non-smoothness, more points should be placed on the region where the control function of the previous solution has steep gradient, and put fewer grid points in the smooth regions. In Step4, the solution for state and control function of the previous iteration is set as the initial guess of the followed iteration. Additionally, the threshold ε is generally set as $\varepsilon = \alpha\,(u_{\max} - u_{\min})$. The main parameters are set as follows:

(1) For the discontinuous optimal control function, α is usually chosen as 0.005∼0.01; for the smooth optimal control function, α is usually chosen as 0.001∼0.005.

(2) For the most problems, $J_{\max}$ should be no great than 10, corresponded finest mesh points is 1025.

The schematic of the proposed method, called AWC for optimal control (AWC-OC) is shown in Figure 5.

IV. NUMERICAL EXAMPLES

Several examples are solved using the second-generation wavelet-based mesh adaptation method. All of the examples demonstrated in this section are taken from the open literature and were solved using the Runge-Kutta discretization. SNOPT [23] is employed as the NLP solver, and automatic differential toolkit Intlab [24] is used to compute the Jacobian matrix. All computations were performed on a computer with Intel (R) Core (TM) i3-2120 CPU 3.30 GHz 3.29 GHz, and 3.48 GB RAM.

A. BREAKWELL PROBLEM

Consider the following minimum-energy problem with a second-order state variable inequality constraint [25]. The problem is to find the control $u(t)$ that minimizes the cost function

$$J = 0.5\int_0^1 u^2 \mathrm{d}t \tag{33}$$

subject to the dynamic constraints

$$\dot{x}(t) = v(t),\ \dot{v}(t) = u(t) \tag{34}$$

the boundary conditions

$$x(0) = 0, x(1) = 0, v(0) = -v(1) = 1 \tag{35}$$

and the state path constraint

$$x(t) \le l \tag{36}$$

where l is a positive real number, x and v are state variables.

The optimal control $u^*(t)$ and optimal index J^* can be given as follows:

(1) $l \ge 1/4$

$$u^*(t) = -2,\ 0 \le t \le 1$$
$$J^* = 2 \tag{37}$$

(2) $1/6 \le l < 1/4$

$$u^*(t) = \begin{cases} -8(1-3l) + 24(1-4l)\,t, & 0 \le t \le 1/2 \\ -8(1-3l) + 24(1-4l)(1-t), & 1/2 < t \le 1 \end{cases}$$
$$J^* = 2 + 6(1-6l)^2 \tag{38}$$

(3) $0 < l < 1/6$

$$u^*(t) = \begin{cases} -\dfrac{2}{3l}\left(1 - \dfrac{t}{3l}\right) & 0 \le t \le 3l \\ 0 \quad 3l < t \le 1-3l & \\ -\dfrac{2}{3l}\left(1 - \dfrac{1-t}{3l}\right) & 1-3l < t \le 1 \end{cases}$$
$$J^* = 4/9l \tag{39}$$

The optimization is started with 17 points and linear initial guess. The threshold of wavelet coefficients is set to $\varepsilon = 1 \times 10^{-3}(u_{\max} - u_{\min})$. The same problem is also solved using the global pseudospectral collocation method with open numerical optimal control codes GPOPS [26]. Both methods were tested on the same computer, and using the same initial guess.

The mesh adaptation history of AWC-OC method for the case with $l = 0.1$ is shown in Figure 6. In the figure, the vertical solid line indicate the points of discontinuities in the analytical solution (at $t = 0.3$ and $t = 0.7$). It is can be seen that the grid points get denser around the two points with discontinuities in the control derivative after each iteration. The state and control function are shown in Figure 7 and 8 respectively. In these figures, the solid lines denote the analytical solution, and the marked lines denote the numerical

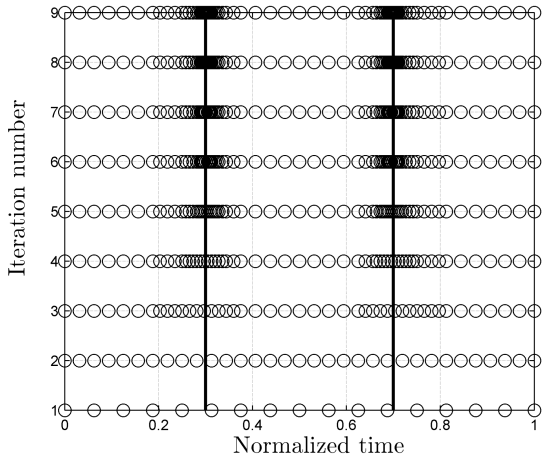

FIGURE 6. Mesh adaptation($l = 0.1$) for Breakwell problem.

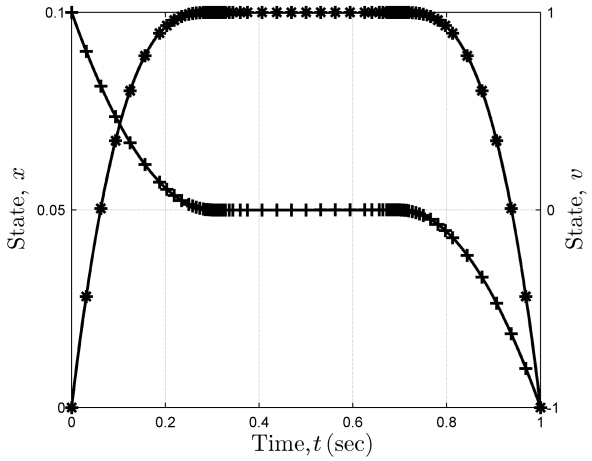

FIGURE 7. Time history of state for Breakwell problem.

TABLE 5. Comparison of precision and optimality.

l	Method	N	$\left\|J-J^*\right\|$	$\left\|u-u^*\right\|_\infty$
0.04	AWC-OC	73	1.12×10^{-8}	2.61×10^{-4}
0.04	GPOPS	89	6.68×10^{-6}	2.35×10^{-2}
0.08	AWC-OC	65	5.61×10^{-9}	1.26×10^{-4}
0.08	GPOPS	50	6.99×10^{-7}	2.96×10^{-2}
0.12	AWC-OC	55	1.01×10^{-7}	1.05×10^{-4}
0.12	GPOPS	56	1.24×10^{-6}	2.55×10^{-2}
0.16	AWC-OC	45	2.80×10^{-9}	4.06×10^{-6}
0.16	GPOPS	43	7.47×10^{-7}	2.00×10^{-2}

solution. The line marked as "$*$" and "$+$" represent the state "x" and "v" respectively.

Table 5 gives the results from AWC-OC and GPOPS for the Breakwell problem. In the table, N is the number of the final mesh, $J - J^*$ is the optimality error, and $\|u - u^*\|_\infty = \max_i |u_i - u^*(t_i)|$ is the norm of the error between the discretized control $\{u_i\}_{i=1}^N$ and the exact solution u^*. The results showed that the optimality error of the GPOPS solution was about $10^{-6} \sim 10^{-7}$ with a maximum control error about 10^{-2}. AWC-OC method exhibited an optimality error at the order $10^{-7} \sim 10^{-9}$, and a maximum control error at the order of $10^{-3} \sim 10^{-4}$. The compared results showed that AWC-OC method proposed in this paper achieved a higher accurate solution than global pseudospectral collocation method by GPOPS.

B. MOON-LANDER PROBLEM

Consider the following optimal control problem, which is known in the literature as the moon-lander problem [9], [27].

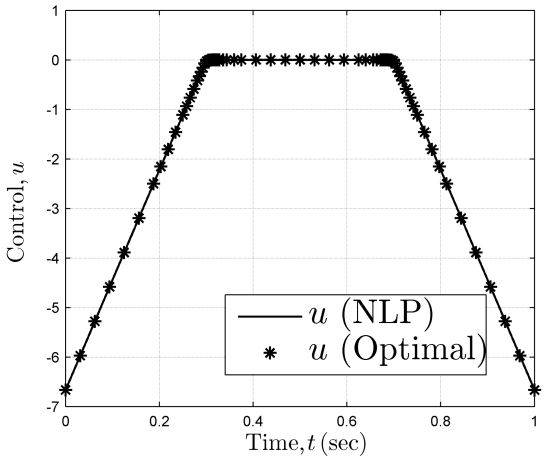

FIGURE 8. Time history of control for Breakwell problem.

The problem is to find the time duration t_f and control $u(t) \in [0, t_f]$ to minimize the cost function

$$J = \int_0^{t_f} u(t)\, dt \tag{40}$$

subject to the dynamic constraints

$$\begin{aligned} \dot{h} &= v \\ \dot{v} &= -g + u \end{aligned} \tag{41}$$

the boundary conditions

$$\begin{aligned} h(0) &= h_0 = 10, \quad v(0) = v_0 = -2 \\ h(t_f) &= h_f = 0, \quad h(t_f) = v_f = 0 \end{aligned} \tag{42}$$

and the control path constraint

$$0 \le u \le u_{\max} = 3 \tag{43}$$

where t_f is free, h and v are state variables, g is a constant, and is equal 1.5. The optimal solution to the moon-lander problem is "bang-bang" type with its minimum value for

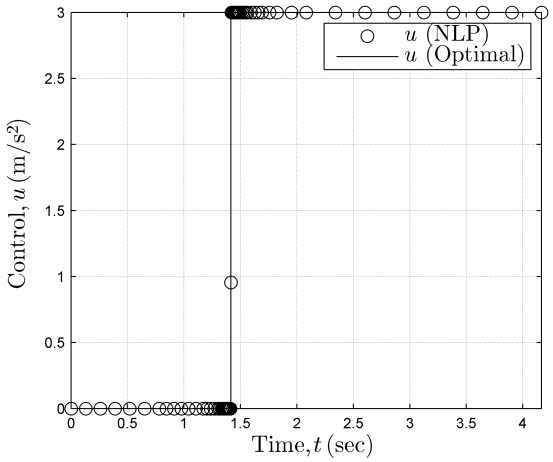

FIGURE 9. The history of control on final grid.

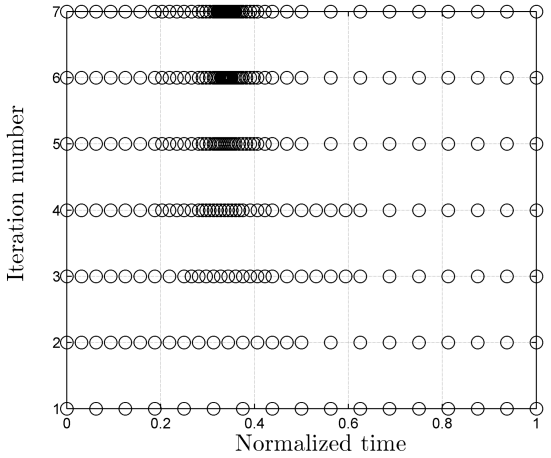

FIGURE 10. Normalized points on various grids.

$t < s^*$ and its maximum value for $t > s^*$, and given as

$$\begin{aligned}&\left(v^*(t), u^*(t)\right)\\ &\quad=\begin{cases}\left(v_0-gt, 0\right), & t\le s^*\\ \left(\left(v_0-u_{\max}s^*\right)+\left(u_{\max}-g\right)t, u_{\max}\right), & t>s^*\end{cases}\end{aligned} \tag{44}$$

$$\begin{aligned}&h^*(t)\\ &\quad=\begin{cases}-\frac{1}{2}gt^2+v_0t+h_0, & t\le s^*\\ \frac{1}{2}\left(u_{\max}-g\right)t^2+\left(v_0-u_{\max}s^*\right)t+\frac{1}{2}u_{\max}\left(s^*\right)^2\\ \qquad +h_0, & t>s^*\end{cases}\end{aligned} \tag{45}$$

where s^* is given as

$$s^*=\frac{1}{u_{\max}}\left[v_0+\left(u_{\max}-g\right)t_f^*\right] \tag{46}$$

with

$$t_f^*=\frac{v_0}{g}+\frac{1}{g}\sqrt{\frac{u_{\max}}{u_{\max}-g}\left(v_0^2+2h_0g\right)} \tag{47}$$

For the boundary conditions given in Equation (42) with $g = 1.5$, $u_{\max} = 3$, the analytically optimal solutions are $\left(s^*, t_f^*\right)$ =(1.415404, 4.164141) and $J^* = 8.2462$.

Figure 9 shows the time history of control of moon-lander problem for $\varepsilon = 1\times10^3$, and Figure 10 shows the distribution of adaptive points on each iteration of the proposed method. The problem is initialized with 17 uniform points. As the iteration continues, more dense points are located near the control discontinuity. After 7 iterations, the final number of grid points is 67. The numerical optimal solutions are (s^*, t_f^*) = (1.41540, 4.16414), and $J^* = 8.2462$. The AWC-OC gives very precious solution. Then, the same problem is solved by GPOPS with 67 global collocation points. The optimized objective function is 8.24697, and the absolute error is 7.723×10^{-4}. It can be seen that AWC-OC method can get more accurate solution than global pseudospectral collocation method by GPOPS by the same number of collocation points.

C. REORIENTATION OF AN ASTMMETRIC RIGID BODY

Two examples above are typical optimal control problems for testing mesh adaptation method. In this subsection, a more complex example taken from engineering is solved by AWC-OC.

Consider the following optimal control problem of reorientation of an asymmetric rigid body [7], [28]. The problem is to find the control $u(t)$ that minimizes the cost function

$$J=t_f \tag{48}$$

subject to the dynamic constraints

$$\begin{aligned}\dot\sigma_1&=\frac{1}{4}\Big(\left(1+\sigma_1^2-\sigma_2^2-\sigma_3^2\right)\omega_1+2(\sigma_1\sigma_2-\sigma_3)\omega_2\\ &\qquad+2(\sigma_1\sigma_3+\sigma_2)\omega_3\Big)\\ \dot\sigma_2&=\frac{1}{4}\Big(2\left(\sigma_1\sigma_2+\sigma_3\right)\omega_1+(1-\sigma_1^2+\sigma_2^2-\sigma_3^2)\omega_2\\ &\qquad+2(\sigma_2\sigma_3-\sigma_1)\omega_3\Big)\\ \dot\sigma_3&=\frac{1}{4}\Big(2\left(\sigma_1\sigma_3-\sigma_2\right)\omega_1+2(\sigma_2\sigma_3+\sigma_1)\omega_2\\ &\qquad+(1-\sigma_1^2-\sigma_2^2+\sigma_3^2)\omega_3\Big)\\ \dot\omega_x&=\left[u_1+(J_y-J_z)\omega_y\omega_z\right]/J_x\\ \dot\omega_y&=\left[u_2+(J_z-J_x)\omega_x\omega_z\right]/J_y\\ \dot\omega_z&=\left[u_3+(J_x-J_y)\omega_x\omega_y\right]/J_z\end{aligned} \tag{49}$$

the boundary conditions

$$\begin{aligned}\sigma^T(0)&=[0,0,0]\\ \sigma^T\left(t_f\right)&=\left[\tan\frac{\phi}{4},0,0\right]\\ \omega(0)&=\omega\left(t_f\right)=0\end{aligned} \tag{50}$$

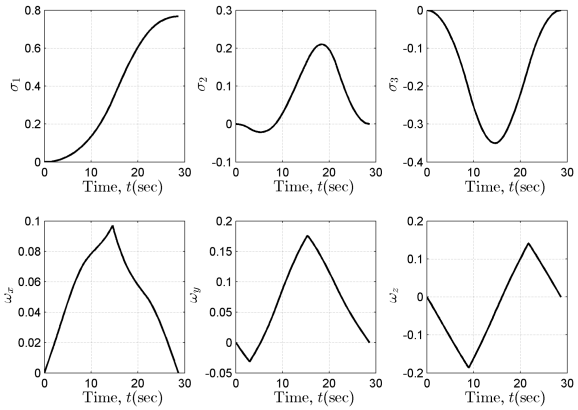

FIGURE 11. Time history of modified Rodrigoues parameter and angular velocity.

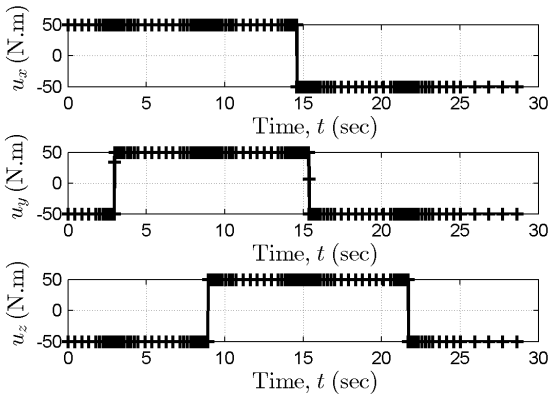

FIGURE 12. Time history of the control torque.

and the inequality path constraint

$$|u_i| \leq 50\text{N} \cdot \text{m} \tag{51}$$

where $\sigma^T = [\sigma_1, \sigma_2, \sigma_3]^T = \tan\frac{\phi}{4}[e_1, e_2, e_3]^T$ is the modified Rodrigues parameters (MRPs), where e_1, e_2, and e_3 are the components of the Euler axis vector, ϕ is the Euler axis rotational angle, $\omega^T = [\omega_1, \omega_2, \omega_3]$ is angular velocity vector. The moments of inertia are given by: $J_x = 5621\,\text{kg}\cdot\text{m}^2$, $J_y = 4547\,\text{kg}\cdot\text{m}^2$, $J_z = 2364\,\text{kg}\cdot\text{m}^2$, the Euler axis rotational angle is $\phi = 150^\circ$.

The problem is initialized with 17 uniform points, after seven iterations, the final number of grid points is 187. The thresholds for wavelet coefficients is $\varepsilon_i = 5 \times 10^2 \|u_{i\max} - u_{i\min}\|$ $(i = 1, 2, 3)$. Figure 11 shows the time history of modified Rodrigoues parameter and angular velocity, Figure 12 shows the time history of control, Figure 13 shows the distribution of adaptive points after each iteration of the method. The optimization objective function is 28.630408. The results are in good agreement with the reference [7]. It can be seen from the results that the mesh points get denser around the control discontinuity by using the mesh adaptation method based on second-generation wavelet.

It is noted that, the dimension of control is three, and the controls are independent each other for this problem. In the process of mesh adaptation, the mesh grids of each control

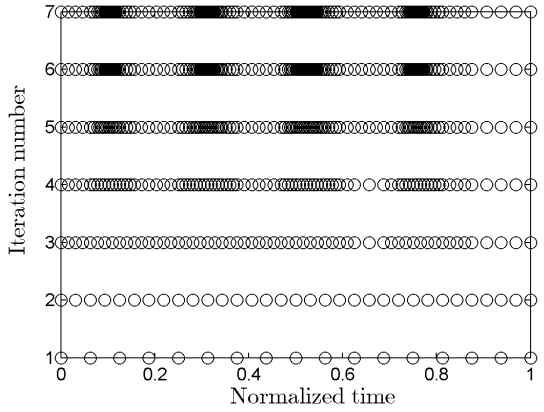

FIGURE 13. Normalized points on various grids.

are computed individually, and then combining the mesh grids. Therefore, there exists denser mesh in smooth region of control.

V. CONCLUSION

In this paper, a second-generation wavelet-based mesh adaptation method (AWC-OC) has been developed for numerically solving the optimal control problems. The Runge-Kutta discretization method is employed to convert the optimal control problem to nonlinear programming (NLP) problem, which can be solved by using standard nonlinear programming codes. To improve the solution accuracy of the optimal control problem, a sequentially iteration solving process is adopted. The non-uniform grid from the background uniform dyadic grids is determined by the proposed method.

The method has been applied to several examples having varying complexity. It can be seen that the method produces solutions with better accuracy than the global pseudospectral method. The method is demonstrated on a wide variety of applications, i.e. non-smooth solution and practical engineering optimal control problems.

REFERENCES

[1] J. Xi, C. Wang, H. Liu, and L. Wang, "Completely distributed guaranteed-performance consensualization for high-order multiagent systems with switching topologies," *IEEE Trans. Syst., Man, Cybern. Syst.*, vol. 49, no. 7, pp. 1338–1348, Jul. 2019.

[2] J. Xi, M. He, H. Liu, and J. Zheng, "Admissible output consensualization control for singular multi-agent systems with time delays," *J. Franklin Inst.*, vol. 353, no. 16, pp. 4074–4090, Nov. 2016.

[3] J. T. Betts, "Survey of numerical methods for trajectory optimization," *J. Guid. Control Dyn.*, vol. 21, no. 2, pp. 193–207, Mar./Apr. 1998.

[4] H. B. Keller, *Numerical Solution of Two Point Boundary Value Problems*, Waltham: Blaisdell, U.K., 1968.

[5] O. von Stryk, "Numerical solution of optimal control problems by direct collocation," in *Optimal Control* (ISNM International Series of Numerical Mathematics), vol. 111, R. Bulirsch, A. Miele J. Stoer, and K. Well, Eds. Basel, Switzerland: Birkhäuser Basel, 1993.

[6] M. A. Patterson and A. V. Rao, "GPOPS-II: A MATLAB software for solving multiple-phase optimal control problems using hp-adaptive Gaussian quadrature collocation methods and sparse nonlinear programming," *ACM Trans. Math. Softw.*, vol. 41, no. 1, p. 1, Oct. 2014.

[7] J. T. Betts, *Practical Methods for Optimal Control and Estimation Using Nonlinear Programming*. Philadelphia, PA, USA: Society for Industrial and Applied Mathematics, 2009.

[8] I. M. Ross and F. Fahroo, "Pseudospectral knotting methods for solving optimal control problems," *J. Guid., Control, Dyn.*, vol. 27, no. 3, pp. 397–405, 2004.
[9] C. L. Darby, W. Hager, and A. V. Rao, "An hp-adaptive pseudospectral method for solving optimal control problems," *Optim. Control Appl. Methods*, vol. 32, no. 4, pp. 476–502, 2011.
[10] F. Liu, W. W. Hager, and A. V. Rao, "Adaptive mesh refinement method for optimal control using nonsmoothness detection and mesh size reduction," *J. Franklin Inst.*, vol. 352, no.10, pp. 4081–4106, Oct. 2015.
[11] S. Jain and P. Tsiotras, "Trajectory optimization using multiresolution techniques," *J. Guid., Control, Dyn.*, vol. 31, no. 5, pp. 1424–1436, 2008.
[12] Y. Zhao and P. Tsiotras, "Density functions for mesh refinement in numerical optimal control," *J. Guid., Control, Dyn.*, vol. 34, no. 1, pp. 271–277, Feb. 2011.
[13] L. Xiao, L. Lv, P. Liu, X. Liu, and G. Huang, "A novel adaptive Gauss pseudospectral method for nonlinear optimal control of constrained hypersonic re-entry vehicle problem," *Int. J. Adapt. Control Signal Process.*, vol. 32, no. 9, pp. 1243–1258, Sep. 2018.
[14] K. Lee, W. H. Moase, and C. Manzie, "Mesh adaptation in direct collocated nonlinear model predictive control," *Int. J. Robust Nonlinear Control*, vol. 28, no. 15, pp. 4624–4634, Oct. 2018.
[15] L. Xiao, P. Liu, X. Liu, Z. Zhang, Y. Wang, C. Yang, W. Gui, X. Chen, and B. Zhu, "Sensitivity-based adaptive mesh refinement collocation method for dynamic optimization of chemical and biochemical processes," *Bioprocess Biosyst. Eng.*, vol. 40, no. 9, pp. 1375–1389, Sep. 2017.
[16] O. V. Vasilyev and C. Bowman, "Second-generation wavelet collocation method for the solution of partial differential equations," *J. Comput. Phys.*, vol. 165, no. 2, pp. 660–693, Dec. 2000.
[17] J. Z. Ben-Asher, *Optimal Control Theory with Aerospace Applications*. Reston, VA, USA: American Institute of Aeronautics and Astronautics, Inc., 2009.
[18] J. C. Butcher, "Implicit Runge-kutta processes," *Math. Comput.*, vol. 18, no. 85, pp. 50–64, 1964.
[19] A. L. Dontchev, W. W. Hager, and V. M. Veliov, "Second-order Runge–Kutta approximations in control constrained optimal control," *SIAM J. Numer. Anal.*, vol. 38, no. 1, pp. 202–226, 2000.
[20] W. W. Hager, "Runge-Kutta discretizations of optimal control problems," in *System Theory: Modeling, Analysis and Control*, T. E. Djaferis and I. C. Schick, Eds. Norwell, MA, USA: Kluwer, 2000.
[21] W. W. Hager, "Runge-Kutta methods in optimal control and the transformed adjoint system," *Numerische Math.*, vol. 87, no. 2, pp. 247–282, Dec. 2000.
[22] W. Sweldens, "The lifting scheme: A construction of second generation wavelets," *SIAM J. Math. Anal.*, vol. 29, no. 2, pp. 511–546, 1998.
[23] P. E. Gill, W. Murray, and M. A. Saunders, "SNOPT: An SQP algorithm for large-scale constrained optimization," *SIAM Review*, vol. 47, no. 1, pp. 99–131, 2002.
[24] S. M. Rump, "INTLAB—INTerval LABoratory," in *Developments in Reliable Computing*, T. Csendes, Ed. Dordrecht, The Netherlands: Kluwer,1999, pp. 77–104.
[25] A. E. Bryson and Y.-C. Ho, *Applied Optimal Control*. New York, NY, USA: Taylor & Francis, 1975.
[26] A. V. Rao, D. A. Benson, C. Darby, M. A. Patterson, C. Francolin, I. Sanders, and G. T. Huntington, "Algorithm 902: Gpops, a MATLAB software for solving multiple-phase optimal control problems using the gauss pseudospectral method," *ACM Trans. Math. Softw.*, vol. 37, no. 2, p. 22, 2010.
[27] J. Meditch, "On the problem of optimal thrust programming for a lunar soft landing," *IEEE Trans. Autom. Control*, vol. 9, no. 4, pp. 477–484, Oct. 1964.
[28] A. Fleming, P. Sekhavat, and I. M. Ross, "Minimum-time reorientation of a rigid body," *J. Guid., Control, Dyn.*, vol. 33, no. 1, pp. 160–170, 2010.

ZHIWEI FENG was born in Linfen, Shanxi, China, in 1984. He received the B.S. degree in aerospace engineering, and the M.S. and Ph.D. degrees in mechanics from the National University of Defense Technology, Changsha, in 2006, 2008, and 2014, respectively, where he has been a Lecturer, since 2014. His research interests include aerodynamic design and multiobjective optimization of flight vehicles.

QINGBIN ZHANG was born in Datong, Shanxi, China, in 1975. He received the B.S., M.S., (mechanics), and Ph.D. degrees in aeronautical and astronautical science and technology from the National University of Defense Technology, Changsha, in 1996, 1999, and 2003, respectively, where he was a Lecturer, from 2003 to 2005, and also an Associate Professor, from 2005 to 2019. Since 2019, he has been a Professor with the National University of Defense Technology. His research interests include multiobjective optimization, space nets, and parachute deployment.

JIANQUAN GE was born in Anshan, Liaoning, China, in 1981. He received the B.S. degree in engineering mechanics from the Dalian University of Technology, Dalian, in 2002, and the M.S. degree in general mechanics and the Ph.D. degree in aeronautical and astronautical science and technology from the National University of Defense Technology, Changsha, in 2004 and 2010, respectively. From 2010 to 2019, he was a Lecturer with the National University of Defense Technology, where he has been an Associate Professor, since 2019. His research interest includes overall design and optimization of flight vehicles.

WUYU PENG was born in Mianyang, Sichuan, China, in 1990. He received the B.S. degree in weapons systems and engineering from the Nanjing University of Science and Technology, Nanjing, in 2012, and the M.S. degree in aeronautical and astronautical science and technology from the National University of Defense Technology, Changsha, in 2015. From 2008 to 2012, he was a student with the Nanjing University of Science and Technology. Since 2012, he has been a student with the National University of Defense Technology. His research interest includes overall design and optimization of flight vehicles.

TAO YANG was born in Changde, Hunan, China, in 1962. He received the B.S. and M.S. degrees in solid rocket engine technology from the National University of Defense Technology, Changsha, in 1989, and the Ph.D. degree in ballistics from the Nanjing University of Science and Technology, Nanjing, in 1992. From 1992 to 1994, he was a Lecturer with the National University of Defense Technology, and was also an Associate Professor, from 1994 to 2001. Since 2001, he has been a Professor with the National University of Defense Technology. His research interests include overall design and optimization of flight vehicles, and aerospace propulsion theory and engineering.

JINLIANG JIE was born in Yichun, Jiangxi, China, in 1983. He received the B.S. degree in materials science and engineering and the M.S. degree in energetic material from the National University of Defense Technology, Changsha, in 2006 and 2008, respectively, where he has been an Engineer, since 2008. His research interests include energetic material and overall design of flight vehicles.